





Open Archive TOULOUSE Archive Ouverte (OATAO)

OATAO is an open access repository that collects the work of Toulouse researchers and makes it freely available over the web where possible.

This is an author-deposited version published in : <http://oatao.univ-toulouse.fr/>
Eprints ID : 20194

To link to this article : DOI:10.1016/j.electacta.2018.01.115
URL : <https://doi.org/10.1016/j.electacta.2018.01.115>

To cite this version : Touzé, Ewen and Gohier, Frédéric and Daffos, Barbara  and Taberna, Pierre-Louis  and Cougnon, Charles
Improvement of electrochemical performances of catechol-based supercapacitor electrodes by tuning the redox potential via different-sized O-protected catechol diazonium salts. (2018) *Electrochimica Acta*, vol. 265. pp. 121-130. ISSN 0013-4686

Any correspondence concerning this service should be sent to the repository administrator: staff-oatao@listes-diff.inp-toulouse.fr

Improvement of electrochemical performances of catechol-based supercapacitor electrodes by tuning the redox potential via different-sized O-protected catechol diazonium salts

Ewen Touzé^a, Frédéric Gohier^a, Barbara Daffos^{b, c}, Pierre-Louis Taberna^{b, c}, Charles Cougnon^{a, *}

^a Laboratoire MOLTECH-Anjou, Université d'Angers, UMR CNRS 6200, 2 bd Lavoisier, 49045, Angers Cedex, France

^b CIRIMAT, Université de Toulouse, UMR CNRS 5085, INPT, UPS, 118 Route de Narbonne, 31062, Toulouse Cedex 09, France

^c Réseau sur le Stockage Electrochimique de l'Energie (RS2E), FR CNRS 3459, 33 Rue Saint Leu, 80039, Amiens Cedex, France

A B S T R A C T

Two different O-protected catechol diazonium salts were synthesized and reacted with microporous Norit-S50 carbon to investigate the impact of the protecting group on the electrochemical performances of supercapacitor electrodes in 1 M H₂SO₄. Carbon products were characterized by thermal gravimetric analysis (TGA), X-ray photoelectron spectroscopy (XPS) experiments and nitrogen gas adsorption-desorption measurements to investigate the film composition, as well as the impact of the grafting on the textural properties of the Norit-S50. Supercapacitor electrodes, prepared from carbon products, were studied by cyclic voltammetry at different scan rates and by galvanostatic charge/discharge experiments after deprotection of catechol-attached groups. It was found that the specific charge was improved by introducing catechol groups under protected forms and that the potential at which the redox reaction occurred depends on the protecting group used. With bulky triisopropylsilyl protecting groups, the formal potential of catechol-attached moieties shifted in the positive direction by about 300 mV, yielding an energy gain significantly increased, compared to the same charge stored in the level of catechol groups introduced with methyl protecting groups. 1100 repetitive charge/discharge curves at 1 A g⁻¹ were achieved to study the stability of supercapacitors electrodes. Results obtained were tentatively explained in terms of the porous structure of the carbon.

Keywords:

Energy
Supercapacitors
Diazonium salts
Microporous carbon
Catechol

1. Introduction

Faradaic-based systems for pseudosupercapacitors are touted for their charge storage and power potentialities, promoted by a reversible surface redox reaction [1,2]. In particular, carbon electrodes grafted with small redox molecules have been proposed to increase capacitance beyond the double-layer charge storage process, while avoiding the release of molecules towards liquid electrolytes [3–16]. Despite a growing interest in this field, these carbon-molecules hybrid systems suffer from a low energy density delivery at the discharge, due to the redox potential often located far away from the electrochemical stability limits of the liquid electrolytes. In contrast to capacitive systems, the design of

faradaic materials at a molecular scale is a promising direction to tackle this issue. A proper selection of electroactive molecules allows maximizing the energy stored in the system by positioning their formal potential near to the low or high limit of the potential window, because the energy increases with the square of the voltage. This is especially true for dual-redox asymmetric systems where both positive and negative electrodes are modified, because the electrochemical storage at the level of molecules ideally should occur with high voltage swings [17–20]. Different approaches have been developed to predict the formal potential of molecules and identify promising candidates for storage applications [21–24]. It was found that addition of aromatic rings, electron-donating or electron-withdrawing groups and heteroatoms have an impact on the formal potential of redox molecules. However, the preparation of selected molecules is rapidly becoming expensive and time consuming. Importantly, it is well-known that the location of the peak potential in cyclic voltammetry depends also on the relative

strength of the adsorption of oxidized and reduced forms of redox molecules. Accordingly, when an electroactive molecule is grafted on porous carbons, a strong anisotropy in surface reactivity contributes to the characteristic multi-peak cyclic voltammograms [18,25]. In the literature, such splitting of the peak potential is often attributed to the presence of different energetically favorable binding surface sites due to the presence of different chemical surface functionalities or structural defects, especially for the catechol unit that is expected to diffuse into the pores [26–30]. In the cyclic voltammograms of catechol-modified porous carbon electrodes, two major pairs of symmetric peaks typically separated by about 200 mV are generally obtained [28–30]. In these studies, the first reversible electrochemical system at lowest potentials was attributed to molecules introduced within the microporous surface, while the reversible system shifted in the positive direction corresponds to molecules located outside of the microporosity. By assuming that it could be possible to selectively introduce molecules on the external surface, this splintering of the peak potential could be a simple and universal remedial solution to the limitations of energy density for supercapacitors, especially in aqueous electrolytes where the electrochemical stability potential window is limited.

Here, we propose to prevent molecules from entering into the micropore structure of the carbon by increasing the relative size of catechol moieties with encumbering substituents, in order to obtain a redox material modified only on the outer surface where molecules are redox active at the higher potential after deprotection. This protection/deprotection strategy will be illustrated with methyl and silyl protective groups due to their facile electrochemical deprotection [9,31]. Catechol derivatives were immobilized on the microporous Norit carbon by spontaneous reaction with the corresponding diazonium salts and carbon products were characterized by TGA analysis, XPS experiments and nitrogen gas adsorption-desorption measurements in order to provide information about the film composition, as well as the impact of the grafting on the textural properties of the porous carbon. Supercapacitor electrodes prepared from carbon products were studied by cyclic voltammetry and galvanostatic charge/discharge experiments in aqueous electrolyte in order to study the impact of the protecting group on their performances.

2. Experimental

2.1. Reagents and surfaces

3,4-dimethoxyaniline (98%) was purchased from Alfa Aesar, 4-

nitrocatechol (97%), triisopropylsilyl chloride (97%), boron trifluoride etherate ($\geq 46\%$ BF₃ basis) and boron tribromide ($\geq 99.99\%$) from Aldrich, imidazole ($\geq 95\%$) from Fluka and tert-butyl nitrite (90%) was received from ACROS. Tetrabutylammonium hexafluorophosphate (Aldrich) and acetonitrile (HPLC grade, Carlo Erba) were used as received. Carbon powder (Norit-S50) was obtained from Norit. Glassy carbon (GC) electrodes from Bioanalytical Systems Inc. (model MF-2012; 3 mm in diameter) were used for cyclic voltammetry.

2.2. Synthesis of aryldiazonium salts

The general procedure for the synthesis of aryldiazonium salts is described in Scheme 1 and follows synthetic routes previously published [32,33].

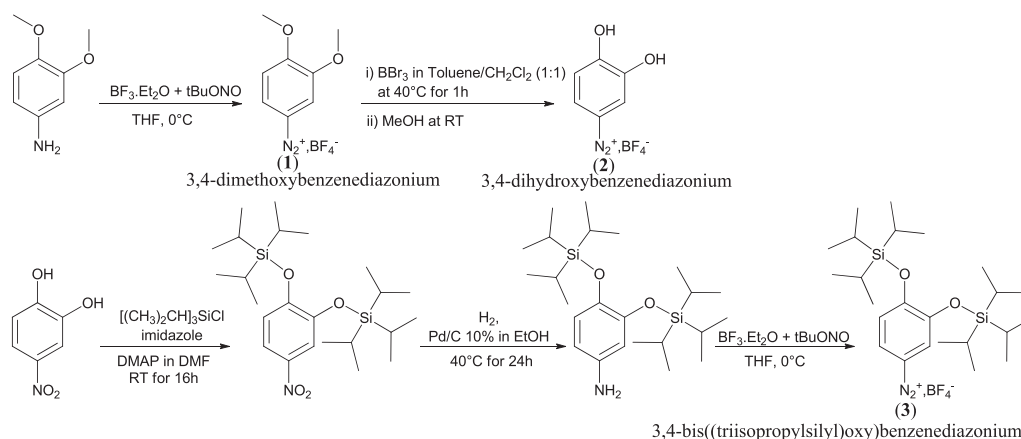
3,4-dimethoxybenzenediazonium tetrafluoroborate (1). Boron trifluoride etherate (9.79 mmol, 1.5 equiv.) was added to a solution of 3,4-dimethoxyaniline (6.53 mmol, 1 equiv.) in 20 mL of THF at an ice bath temperature. After 5 min stirring, tert-butyl nitrite (7.83 mmol, 1.2 equiv.) was added drop wise at 0 °C. After 15 min stirring, the precipitated was filtered and washed with diethyl ether to afford the diazonium salt in 90% yield as a black powder.

¹H NMR (300 MHz, (CD₃)₂CO, TMS): δ = 8.55 (dd, ³J (H,H) = 9.1 Hz, ⁴J (H,H) = 2.5 Hz, 1H), 8.22 (d, ⁴J (H,H) = 2.5 Hz, 1H), 7.56 (d, ³J (H,H) = 9.0 Hz, 1H), 4.17 (s, 3H), 3.99 (s, 3H). ¹³C NMR (100 MHz, (CD₃)₂CO): δ = 161.7, 151.2, 131.9, 114.4, 113.4, 103.2, 57.8, 57.3.

3,4-dihydroxybenzenediazonium tetrafluoroborate (2). 3,4-dimethoxybenzenediazonium tetrafluoroborate (1) (1 mmol, 1 equiv.), was dissolved in 3 mL of toluene under argon atmosphere. Then 1 M boron tribromide in CH₂Cl₂ (3 mmol, 3 equiv) was slowly added at room temperature to the solution and the mixture was stirred for 1 h at 40 °C. After cooling, MeOH (1 mL) was added. After 5 min stirring, the mixture was concentrated under reduced pressure to give a dark residue, which was recrystallized from methanol/ether. The product was obtained in 84% yield as a brown powder.

¹H NMR (300 MHz, D₂O, TMS): δ = 8.06 (dd, ³J (H,H) = 9.0 Hz, ⁴J (H,H) = 2.6 Hz, 1H), 7.79 (d, ⁴J (H,H) = 2.6 Hz, 1H), 7.18 (d, ³J (H,H) = 9.0 Hz, 1H). ¹³C NMR (100 MHz, (CD₃)₂CO): δ = 161.9, 148.9, 130.7, 118.9, 117.3, 100.1.

3,4-bis((triisopropylsilyloxy)benzenediazonium tetrafluoroborate (3). A solution of 4-nitrocatechol (7.48 g, 1 equiv.), triisopropylsilyl chloride (18.67 mmol, 2.5 equiv.), imidazole (19.10 mmol, 2.55 equiv.) and dimethylaminopyridine (DMAP; 0.67 mmol, 0.1 equiv.) in DMF (36 mL) was stirred at room



Scheme 1. General procedure for the synthesis of diazonium salts.

temperature for 16 h. The reaction solution was poured into water (50 mL) and extracted with EtOAc (2×50 mL). The organic layers were combined and washed with water (2×50 mL), dried over Na_2SO_4 , filtered and concentrated under vacuum to an orange oil. The crude reaction mixture was purified via SiO_2 chromatography (gradient 0–10% EtOAc in hexane) to afford the triisopropylsilyl protected nitrocatechol as a pale yellow solid in 86% yield. A suspension of triisopropylsilyl protected nitrocatechol (5.99 mmol, 1 equiv.) and 10% palladium on carbon (0.64 g, 0.60 mmol) in ethanol (40 mL) was evacuated and flushed with hydrogen gas (1 atm). The suspension was stirred under nitrogen atmosphere for 24 h at 40°C . The reaction mixture was then evacuated, flushed with argon and then filtered through celite (50 g) with dichloromethane (200 mL). The filtrate was concentrated under vacuum and the resulting crude oil was purified via SiO_2 with dichloromethane to afford compound **3** in 75% yield as a yellow solid. ^1H NMR (300 MHz, $(\text{CD}_3)_2\text{CO}$, TMS): $\delta = 7.45$ (d, $^3J(\text{H,H}) = 9.0$ Hz, 1 H), 6.96 (d, $^3J(\text{H,H}) = 9.0$ Hz, 1 H), 6.13 (s, 1 H), 1.31 (m, 36 H). ^{13}C NMR (75 MHz, CDCl_3): $\delta = 162.4, 145.8, 130.9, 120.3, 118.4, 99.2, 17.2, 11.7$.

2.3. Chemical modification of glassy carbon and activated carbon

Before modification, glassy carbon electrodes were polished using $0.04\ \mu\text{m}$ alumina and next, sonicated in water and acetonitrile. Glassy carbon working electrodes were electrochemically modified in 1 mM acetonitrile solutions of diazonium salts +0.1 M Bu_4NPF_6 by recording 10 successive cyclic voltammograms (CVs) from 0 V to -0.7 V vs. Ag/AgNO_3 at $100\ \text{mV s}^{-1}$. After sonication in acetonitrile and water, modified electrodes were studied by cyclic voltammetry at $100\ \text{mV s}^{-1}$ in 0.1 M H_2SO_4 . In aqueous electrolyte, the electrode potential is referred to the Ag/AgCl system.

For the modification of the carbon powder, 400 mg of carbon Norit-S50 (NS) was dispersed in 50 mL of acetonitrile by sonication for 30 min and then 1.67 mmol (0.05 equivalent versus carbon) of diazonium salts was added. After stirring at room temperature for 5 h, the reaction mixture was vacuum filtered on a Teflon filtration membrane (from Sartorius Stedim) having a pore size diameter of $0.2\ \mu\text{m}$. Carbon products obtained were thoroughly washed twice with acetonitrile (100 mL), DMF (100 mL), methanol (100 mL) and acetone (100 mL), before to be dried overnight at 80°C .

2.4. Preparation of supercapacitors electrodes

Supercapacitors electrodes were prepared by mixing the active material with polytetrafluoroethylene (PTFE, 60 wt% dispersion in water) used as binder and carbon black (superior graphite) used as conducting additive with a ratio of 75:10:15 (wt; wt; wt) in a small volume of ethanol until a homogeneous carbon paste was obtained. The carbon paste was spread to obtain a thin film which was dried at 80°C for 1 h. A sample of some milligrams was pressed for 60 s at 1 MPa between two stainless steel grids (80 mesh, 0.127 mm, Alfa Aesar) used as current collector.

2.5. Instrumentation

Electrochemical measurements were achieved at room temperature in a three-electrode cell connected to a potentiostat/galvanostat model VSP (from Bio-Logic) monitored by ECLab software. XPS measurements were performed with a Kratos Axis Ultra spectrometer using a Al K_α monochromatic beam working at 1486.6 eV. All spectra were recorded in the constant energy mode at a pass energy of 20 eV. Data treatment was performed with CasaXPS software and all spectra were calibrated taking 284.5 eV (graphite like carbon) as a reference binding energy. Porosity characteristics were calculated from nitrogen sorption isotherms

measured at 77 K using a Micromeritics ASAP 2020 porosimeter. The specific surface area was estimated by using BET, while the pore volumes and the pore size distributions were calculated from adsorption isotherms by using the QSDFT method. TGA analyses were performed using a TA instruments (TGA Q500) apparatus by heating 5 mg typical masses of carbon products in nitrogen atmosphere from 60°C to 1200°C at a rate of $10^\circ\text{C}/\text{min}$. The temperature was maintained at 60°C for 20 min before the experiment starts.

3. Results and discussion

3.1. Spontaneous grafting of the aryldiazonium salts on Norit S50

Fig. 1 shows XPS spectra of the C1s and N1s core levels for unmodified and functionalized Norit carbon products.

Beside a main photoelectron peak at 284.5 eV that is assigned to sp^2 C–C bonds in graphite-like carbon, the C1s XPS spectra of modified carbons show photoemission peaks at higher binding energies, which are attributed to electron deficient carbon atoms. C1s XPS spectra for the Norit carbon modified with the 3,4-dihydroxybenzenediazonium salt and the 3,4-dimethoxybenzenediazonium salt correlate well with two contributions at around 286 eV and 287 eV in addition to the reference peak at 284.5 eV. The peak at 286 eV can be assigned to the C–OH and C–O–C contributions depending on whether catechol or dimethoxybenzene units were introduced [16,34,35]. The peak at 287 eV might originate from carbonyl functionalities present at the surface of the pristine Norit carbon or can provide from partial oxidation of catechol groups [35]. For the Norit carbon modified with the 3,4-bis((triisopropylsilyl)oxy)benzenediazonium salt, two additional contributions were obtained at 283.5 eV and 285.3 eV, which can be attributed to the C–Si bond and sp^3 -hybridized carbons providing to the silyl protecting groups [36]. A peak at 101.5 eV in the XPS spectrum of the Si2p core level also provides evidence of the introduction of bis((triisopropylsilyl)oxy)benzene units (Fig. S1) [37].

The N1s core-level spectra show nitrogen contributions over a wide range of binding energy, corresponding to nitrogen species in high and low oxidation states. Note that the unmodified carbon does not show any nitrogen peaks, confirming that the pristine carbon does not contain detectable nitrogen species. The presence of N1s emission for carbons modified with diazonium salts that do not bear any nitrogen-containing substituent, is frequently reported in literature, proving that the dediazonation step is incomplete during the grafting process [38]. The peak at around 400 eV has been assigned to diazenyl groups resulting to the electrophilic attack of the diazonium cation on the carbon surface or on the phenyl ring of previously attached molecules [38–40]. At 399 eV and 402 eV, two additional peaks were detected, which can be attributed to physisorbed ACN and DMF molecules used as rinsing solvents [41]. At higher binding energies, the presence of two peaks at 404.8 eV and 406.4 eV with an area ratio of 1:1 is characteristic of diazonium groups [42–44]. The peak at the highest binding energy is assigned by Finn and Jolly to the nitrogen atom directly attached to the phenyl group in the diazonium salt [44]. These peaks may be assigned to strongly physisorbed diazonium salts, forming complexes with aromatic structures [45]. This explanation is well supported by the presence of F1s and B1s peaks in the wide XPS survey spectrum of the Norit carbon modified with the 3,4-bis((triisopropylsilyl)oxy)benzenediazonium tetrafluoroborate (Fig. S2).

Importantly, with the silyl protecting groups, the N1s peak attributed to azo-bonds became prominent compared to the other carbon products. This is possibly due to a more efficient formation

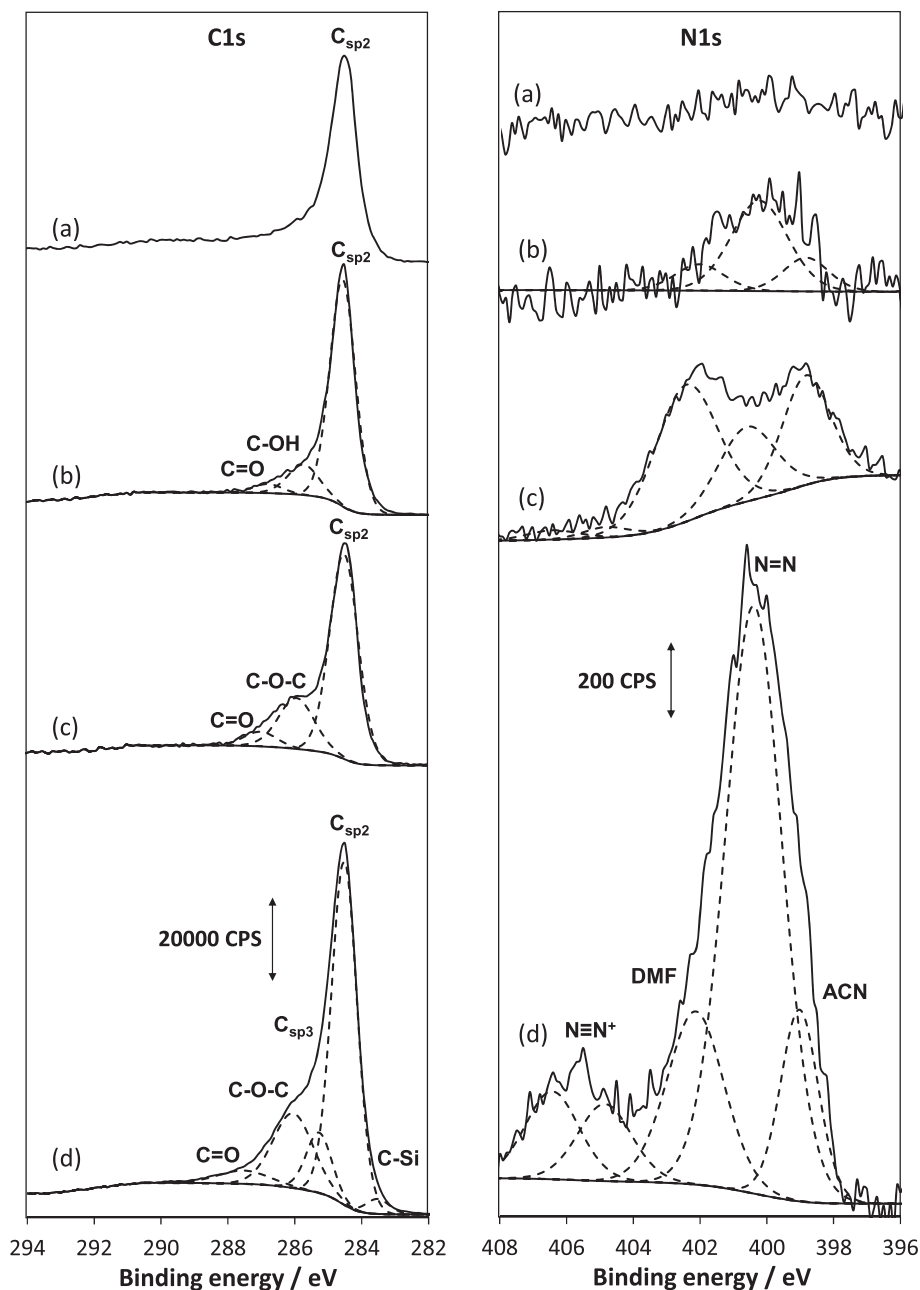


Fig. 1. XPS spectra of C1s and N1s core levels for unmodified (a) and modified Norit carbon with 3,4-dihydroxybenzenediazonium salt (b), 3,4-dimethoxybenzenediazonium salt (c) and 3,4-bis((triisopropylsilyl)oxy)benzenediazonium salt (d).

of azo-bonds with the 3,4-bis((triisopropylsilyl)oxy)benzenediazonium salt. Nevertheless, this seems unlikely to be able to fully account for the very marked differences in the N1s XPS spectra, because the electrophilic attack of diazonium cations is mainly governed by their electronic properties [46], which do not significantly change when the oxygen atoms are protected with methyl or silyl groups. A more tenable explanation is that the molecules protected with bulky silyl groups are selectively introduced on the outer surface of the Norit carbon and become more “visible” by the surface-sensitive XPS measurements [47].

3.2. Electrochemical behavior of modified Norit carbon electrodes

Fig. 2 shows CVs recorded in 1 M H₂SO₄ on Norit carbon electrodes spontaneously modified with the three diazonium salts

studied. Note that before study, the surface-attached molecules were electrochemically deprotected by recording successive CVs in 1 M H₂SO₄ up to 0.8 V until a stabilized CV was obtained [9]. In this way, after deprotection, a catechol-tethered surface is obtained whatever the diazonium salt used. However, the different locations in potential of the electrochemical systems ascribed to the attached-catechol moieties and their relative intensities, indicate a possible effect of the protecting groups on the selectivity and the efficiency of the surface grafting process.

CVs obtained shows two reversible systems separated by about 300 mV, possibly due to catechol moieties in different chemical environments. Nagaoka and Yoshino observed a similar complex CV for the catechol adsorbed on an anodized GC electrode (the anodic treatment creates microporosity) [28]. Authors conclude that the more anodic reversible system corresponds to adsorption

of catechol on the outer surface, while the reversible system shifted towards the negative direction arises from catechol adsorbed on the micropore surface. Authors evoke a favorable π - π interaction between catechol and graphite-like surface of glassy carbon required to enter into the microporosity.

From our results, only the Norit carbon modified with the 3,4-dihydroxybenzenediazonium salt give two well-defined reversible systems of almost equal current intensity (Fig. 2a). After modification with 3,4-dimethoxybenzenediazonium salt, the first reversible system dominates (Fig. 2b), while mainly the second system contributes to the faradaic envelope of the CV recorded with the Norit electrode modified with 3,4-bis((triisopropylsilyl)oxy)benzenediazonium salt (Fig. 2c). These differences can be tentatively explained in terms of the porous structure of the Norit carbon if we assume that the pores diameter is too small for the O-protected catechol diazonium salt with bulky silyl groups, while catechol and dimethoxybenzene derivatives can diffuse in the porous structure.

The total specific charge (Q_T), determined by integrating the area under the CVs presented in Fig. 2 and the faradaic contribution (Q_F) of molecules to the charge storage, deduced by subtracting the double-layer contribution (Q_{dl}) of the carbon, are showed in Table 1 for all carbon products. In addition, determination of the molecule-loading (Γ_{TGA}) by TGA experiments in N_2 atmosphere, gives access to the faradaic efficiency of molecules by assuming that two electrons per molecule were exchanged.

Despite Q_T is improved in all cases after modification, Q_F varies in the order Norit-OTIPS > Norit-OMe > Norit-OH, while the molecular-loading shows the opposite, implying a better faradaic efficiency of molecules for Norit-OTIPS. Note that the double-layer of the Norit carbon is weakly impacted by the grafting whatever the diazonium salt used. With Norit-OTIPS, the more important fraction of molecules involved in the charge storage process is consistent with an improved electrochemical accessibility of molecules, while the important fraction of "silent" molecules with Norit-OH and Norit-OMe can be considered as a "dead mass" due to their isolation in the porous structures of the carbon. To verify this assumption, CVs were recorded at different scan rates comprised between 7 mV s^{-1} and 150 mV s^{-1} . Fig. 3 shows the variation of the total specific charge as a function of scan rate. For the unmodified Norit electrode, a rapid increase of Q_T is noticeable at slow scan rate ($< 20 \text{ mV s}^{-1}$), due to a larger fraction of the specific area accessible to ions at this time scale. For supercapacitor electrodes prepared from Norit-OH and Norit-OMe, Q_T is less influenced by the scan rate in the low scan rate domain, which is indicative of a poorer accessibility of ions to the micropore surface. With the Norit-OTIPS, the scan rate dependence of the total specific charge over the low scan rate domain follows approximately the same trend that for the unmodified Norit electrode, implying that no significant obstruction of porosity occurs during the chemical modification of the carbon. By analogy, a previous work reported by Hapiot et al. may provides guidance for interpretation of the scan rate effect on the specific charge [48]. Authors have demonstrated that the use of diazonium salts with functionalities protected by different-sized groups allows to finely control the structure of a molecular assembly at a surface, obtaining molecules spaced away from each other with a gap created by the release of protecting groups. Especially, the use of bulky protecting groups, such as triisopropylsilyl groups, was found to increase the permeability of the organic layer by creating diffusion channels in the layer after deprotection. In our case, it can be assume that the use of triisopropylsilyl protecting groups improves the electrolyte penetrability in the porous structure of the carbon by avoiding molecules to enter into the micropores of diameter less than the molecular size and by restoring diffusion channel through the layer after deprotection.

However, there is not a clear consensus on which effect (i.e., textural effect or chemical effect) is responsible to the multi-peak features of the CVs. Interestingly, when a glassy carbon electrode polished to a mirror-like appearance was modified by electrochemical reduction in acetonitrile solutions containing the diazonium salts studied, the grafting, which is assumed to occurred by radical attack, produced in all cases a main reversible electrochemical system centered at $0.55 \text{ V vs. Ag/AgCl}$ (Fig. S3), implying that the porous interface could be responsible to the multi-peaks system obtained with modified Norit electrodes. From the similarities between the reversible system obtained with a perfectly flat modified glassy carbon electrode and the second system observed with modified Norit electrodes, it seems reasonable to propose that this latter system can be ascribed to molecules grafted by radical attack on the outer surface or at the micropores entrance. In this way, a tenable explanation for the multi-peak CVs obtained with modified Norit electrodes is that molecules introduced on the internal surface of the porous interface could be responsible for the first reversible system. This explanation is reinforced by a recent work of Downard et al. evoking the possibility of a spontaneous grafting mechanism in two steps, including first the formation of a primer organic layer on the surface by radical attack and second, the further growth of this organic layer by reaction with a solution-generated reactive species [49]. If a similar mechanism operates in this work, a process involving surface attack by radicals can account for the spontaneous grafting reaction at short reaction times.

3.3. Impact of the chemical modification on the textural properties of the Norit carbon

To investigate in detail the impact of the grafting on the textural properties of the Norit carbon, nitrogen gas adsorption-desorption measurements were achieved with unmodified and modified carbons (Fig. 4).

Before chemical modification, the adsorption branch of the isotherm of the Norit carbon presents a net increase in the adsorbed volume at low relative pressure (P/P^0) followed by a nearly horizontal plateau in the intermediate and high P/P^0 values, while the desorption branch of the isotherm retraces nearly the same path. Such N_2 adsorption-desorption isotherms approach a reversible type I isotherm, according to the IUPAC classification, which is typical of a microporous structure [50]. After chemical modification, the adsorption-desorption isotherms of the Norit carbon show a net decrease in the adsorbed volume at low relative pressure. The loss of adsorbed volume is becoming more pronounced with protected molecules and increases in the order Norit-OH < Norit-OMe < Norit-OTIPS. With unprotected catechol, the BET specific surface area reduced from $1699 \text{ m}^2 \text{ g}^{-1}$ to $1349 \text{ m}^2 \text{ g}^{-1}$, while it reduced up to $1158 \text{ m}^2 \text{ g}^{-1}$ and $1113 \text{ m}^2 \text{ g}^{-1}$ with methyl and triisopropylsilyl protective groups, respectively. These results demonstrate that the microporous surface is differently impacted by the grafting, depending on the molecular sizes. Especially, a more important fraction of micropores is suppressed as the molecular size increases, implying that the grafting mainly blocks the microporosity by a steric effect. For better understanding the impact of the grafting on the carbon texture, isotherms were further analyzed by determining the pore size distribution (Fig. 5).

Before chemical modification, the pore size distribution shows that the Norit carbon has mainly micropores ($< 2 \text{ nm}$) with a small fraction of mesopores between 2 and 2.5 nm. After grafting, the pore size distribution in the micropores domain is differently impacted according to the diazonium salt used, while the loss of the mesopores volume is nearly the same. Such results support that the microporosity is responsible to the complex CVs obtained with modified Norit electrodes. Intriguingly, with the bulky silyl

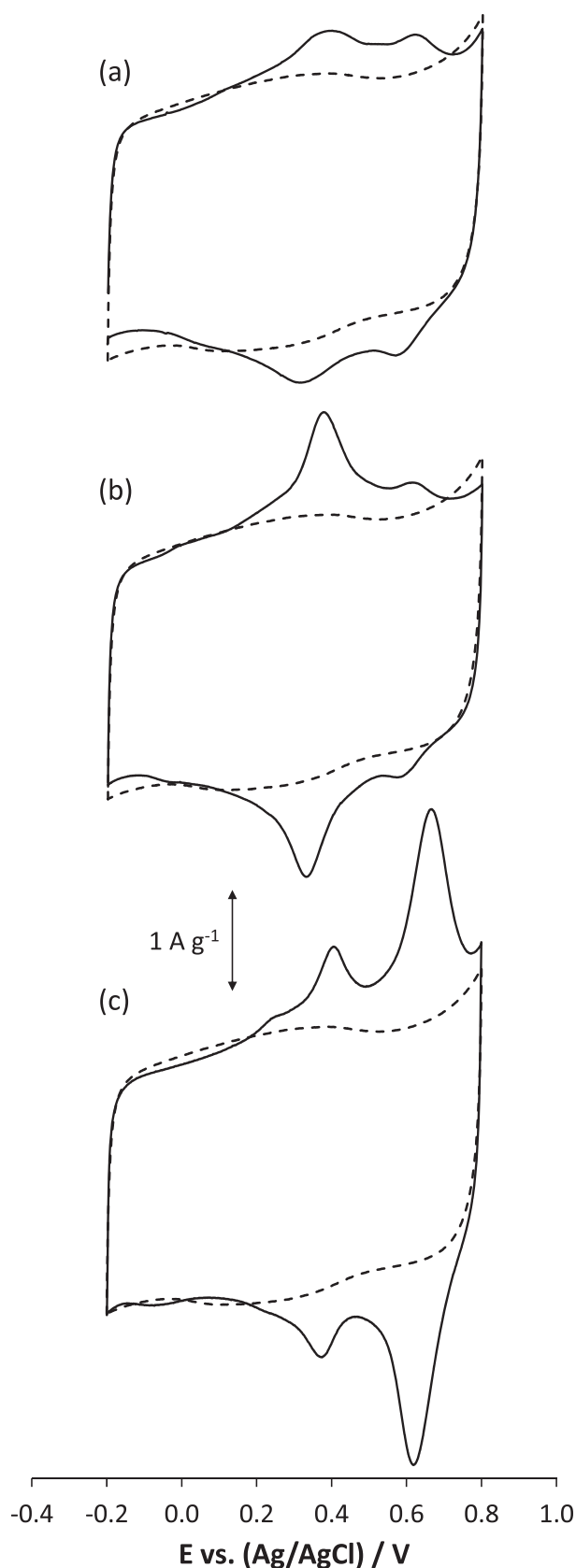


Fig. 2. CVs recorded at 10 mV s^{-1} in $1 \text{ M H}_2\text{SO}_4$ with unmodified Norit carbon electrode (curve in dotted line) and with Norit carbon electrodes modified with 3,4-dihydroxybenzenediazonium salt (a), 3,4-dimethoxybenzenediazonium salt (b) and 3,4-bis((triisopropylsilyl)oxy)benzenediazonium salt (c). The current was normalized with respect to the mass of active material (without organic binder and superior graphite).

protecting groups, the larger micropores with 1.5–2 nm diameter are less impacted by the chemical modification, compared to the methyl protecting groups. Assuming that the accumulation of molecules at the entrance of micropores is responsible to the loss of the microporous volume, an increase in the size of molecules is expected to favor such “constriction” phenomenon [51]. On the contrary, for the mesopores, a progressive coverage of the inner pore surface is expected to give a more progressive decrease of their volume and so, mesopores are expected to be less sensitive to the molecular size. To compare the affected pore region for the two O-protected catechol carbon products, which give a different location in potential for the main reversible system in cyclic voltammetry, the inset of Fig. 5 presents the subtracted pore volume distribution obtained by difference between the pore size distribution for the bis((triisopropylsilyl)oxy)benzene and dimethoxybenzene-modified Norit carbons. Assuming that the accumulation of molecules at the pore entrance is preferred, there is tentative evidence from the data in Fig. 5 that with pores having diameters below 0.6 nm, both the dimethoxybenzene and the bis((triisopropylsilyl)oxy)benzene units are large enough for blocking pores by the grafting of a single molecule at their entrance, while the grafting of silyl protected molecules more efficiently blocks pores with 0.60–1.35 nm diameter. In contrast, pores with diameter larger than 1.35 nm were found to be less obstructed by the bis((triisopropylsilyl)oxy)benzene units, compared to the dimethoxybenzene-modified Norit carbon. These changes fit well with the molecular sizes regarded as the higher interatomic distance between the two protecting groups. Molecular sizes were calculated by Chem3D and found to be 0.59 nm with the methyl groups and 1.2 nm with the silyl groups. In Fig. 6, we propose to normalize the pore size distribution of the Norit carbon by the molecular size. With such normalized pore size distribution, it appears that the Norit carbon has mainly pores with diameters less than two times the size of bis((triisopropylsilyl)oxy)benzene units.

For pores with a diameter corresponding to the size of molecules, accumulation of molecules at their entrance immediately blocs their access to N_2 adsorbate, while pores with normalized diameter comprise between 1 and 2 remain accessible to the adsorbate but do not allow the diffusion of molecules inside the porosity. Only pores with normalized diameter more than 2, can be accessed by molecules and can be possibly modified on their inner surface. Such representation permits to rationalize results and suggests that the porosity must be adapted to the molecular size. With this approach, it would be expected that the 3,4-bis((triisopropylsilyl)oxy)benzenediazonium salt mainly affects the outer surface of the Norit carbon, while the 3,4-dimethoxybenzenediazonium salt can have access to a part of the micropore volume, which can be possibly reduced by a progressive coverage of their inner surface. This explanation supports that the different locations in potential of the reversible electrochemical systems obtained in cyclic voltammetry are mainly due to a textural effect and it was found that a higher energy corresponds to the electric charge stored at the level of molecules grafted at the pores entrance. In this way, this protection/deprotection strategy offers the possibility of matching a more important energy to the faradaic contribution of the electric charge storage by adjusting the molecular sizes to the textural properties of the carbon.

3.4. Impact of the protecting group on the energy density of supercapacitors

In order to evaluate the benefit of the protecting groups on the electrochemical performances of modified-carbon based supercapacitors electrodes, galvanostatic charge/discharge experiments were performed from 0 to 0.8 V at 1 A g^{-1} . Fig. 7A presents the

Table 1
Electrochemical performances of supercapacitors electrodes deduced from CVs at 10 mV s⁻¹.

Carbon products	Q _T (C g ⁻¹)	Q _{dl} (C g ⁻¹)	Q _F (C g ⁻¹)	Γ _{TGA} (mol g ⁻¹) ^a	Faradaic efficiency (%)
Norit	114.6	114.6	—	—	—
Norit-OH	127.1	105.8	21.3	0.00125	8.8
Norit-OMe	136.4	107.9	28.5	0.00078	19.0
Norit-OTIPS	148.9	103.3	45.6	0.00040	59.0

^a The mass fraction of molecules is determined from the global weight loss at 700 °C.

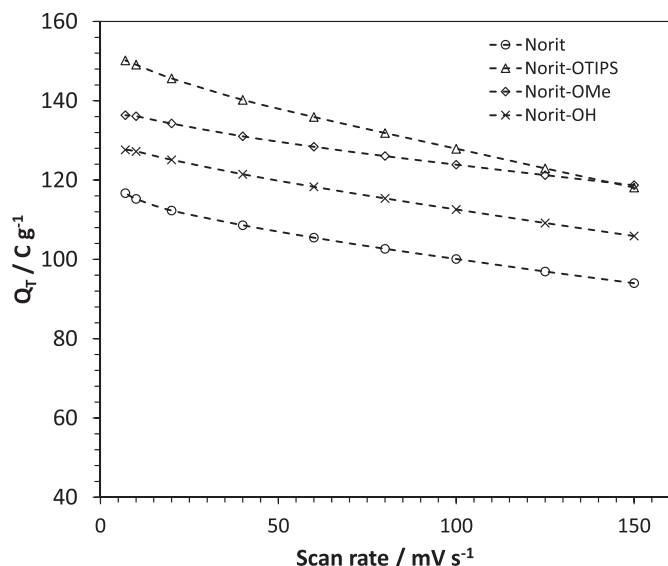


Fig. 3. Evolution of the total specific charge as a function of scan rate for unmodified and modified Norit carbons.

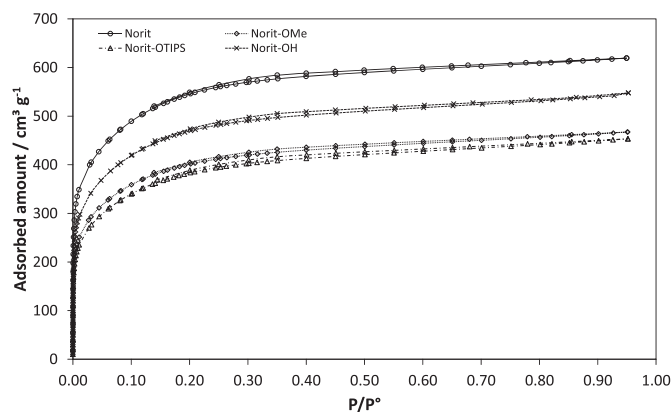


Fig. 4. Adsorption-desorption isotherms of nitrogen at 77 K for unmodified and modified Norit carbons.

discharge curves and Fig. 7B shows the evolution of the total specific charge Q_T deduced to the charge/discharge curves at 1 A g⁻¹ during the first 1100 cycles.

As I × Δt corresponds to the average specific charge, the increase in charge/discharge time for modified carbons is indicative of an increase in the global specific charge. After modification with catechol derivatives a specific charge gain comprised between 20% and 30% is obtained. Note that the two carbon products Norit-OH and Norit-OMe give nearly the same increase in specific charge, while the most significant improvement corresponds to Norit-OTIPS, in good agreement with the CVs. Fig. 7B shows that, in all

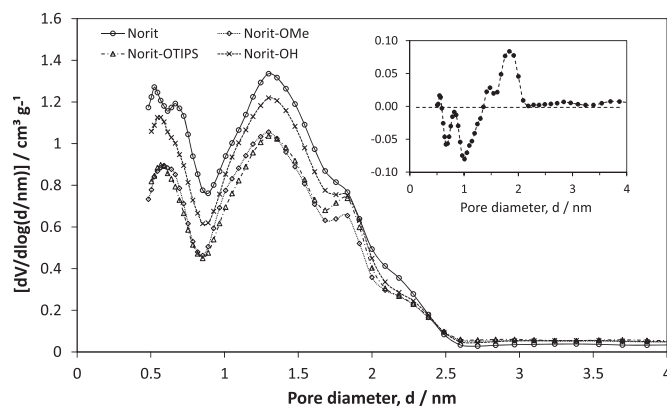


Fig. 5. Pore size distribution of unmodified and modified Norit carbons. The inset shows the subtracted pore volume distribution obtained by difference between the pore size distribution for the bis((triisopropylsilyl)oxy)benzene and dimethoxybenzene-modified Norit carbons.

cases, the specific charge slightly decrease during the first few hundred cycles, due to the departure of just physisorbed molecules from the surface to the liquid electrolyte, and then tends to stabilize after 1000 charge/discharge cycles, indicating that the beneficial effect of the catechol groups remains even after long time cycling. The specific charge retention after 1000 cycles is 89.4% for Norit-OH, 95.4% for Norit-OMe and 89.6% for Norit-OTIPS. Note that carbon products where molecules or a fraction of molecules are suspected to be grafted onto the external surface have depressed charge retentions, probably due to a better contact between molecules and the liquid electrolyte that favours their desorption. For the same reason, the excellent charge retention obtained with Norit-OMe can be explained by a poorer contact between molecules and the liquid electrolyte, due to their isolation in the microporosity.

Importantly, the potential at which the redox reactions occur change depending on the diazonium salt used for the chemical modification. With O-methyl protected catechol moieties, a plateau is clearly visible at around 0.35 V during the discharge, while the discharge of catechol mainly proceed at around 0.65 V when silyl protecting groups are used during the modification step. Note that by using unprotected catechol diazonium salt, the plateau is less well-defined because the two reversible systems have approximately the same current intensity. This change in potential for the faradaic contribution to the charge storage has a profound impact on the energy delivered at the discharge (Fig. 8). More the reversible electrochemical system at higher potential becomes pronounced, more the energy density increases. Whereas there is not much difference between the total specific charges with the two protected-catechol carbon products, the energy gain almost tripled with silyl groups compared to methyl groups, changing from 15% to 40%. These results make the bis((triisopropylsilyl)oxy)benzenediazonium salt a good candidate for the modification of the Norit carbon for charge storage applications and prove that the molecular sizes must be adapted to the textural properties of porous carbons

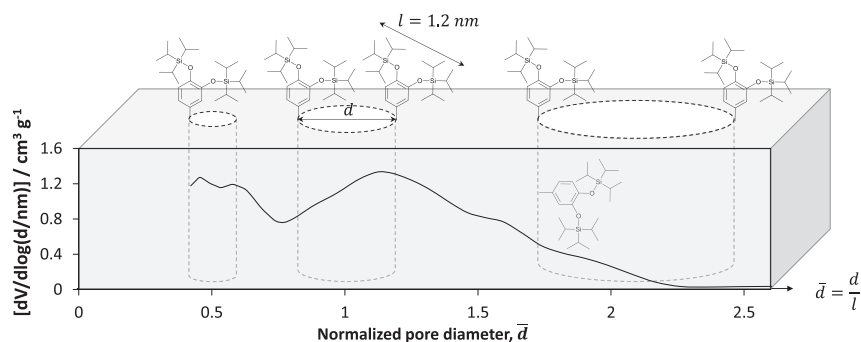


Fig. 6. Schematic representation of the impact of the molecular size on the porous structure of the Norit carbon. In this representation, illustrated with the Norit-OTIPS carbon product, the normalized pore size distribution is obtained by dividing pore diameters d by the molecular size l , which is assumed to be the higher interatomic distance between the two protecting groups calculated by Chem3D.

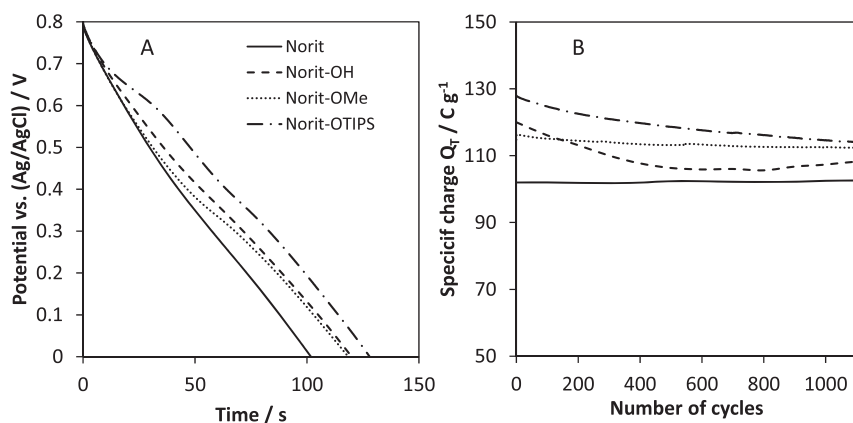


Fig. 7. (A) Discharge curves at 1 A g^{-1} for unmodified and modified Norit carbon electrodes. (B) Evolution of the total specific charge during the first 1100 charges/discharge cycles.

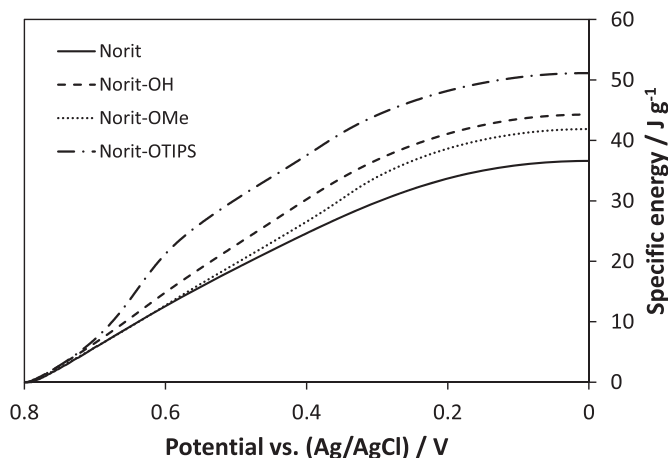


Fig. 8. Specific energy delivered during the discharge at 1 A g^{-1} for unmodified and modified Norit carbon electrodes.

to maximize the performances of carbon-molecules based hybrid storage systems.

4. Conclusion

Two different O-protected catechol diazonium salts were synthesized and introduced on the surface of the Norit-S50 carbon to prepare supercapacitor electrodes working in $1 \text{ M H}_2\text{SO}_4$. The carbon products obtained were characterized by TGA and XPS

experiments. After deprotection, multi-peak systems, mainly composed of two reversible systems separated by around 300 mV , were obtained in cyclic voltammetry. Results show that the relative intensities of these two pairs of symmetric peaks are related to the nature of the protecting group. The role of the protecting group and its impact on the potential at which catechol is electroactive after deprotection were investigated by electrochemical techniques and nitrogen gas adsorption-desorption measurements. The following conclusions can be drawn from results.

- (i) The specific charge was improved by using a O-protected catechol diazonium salt with triisopropylsilyl groups during the modification step.
- (ii) With triisopropylsilyl protecting groups the reversible electrochemical system located at higher potential dominates, while that at lower potential mainly contributes to the multi-peak envelope in the CV when methyl protecting groups are used.
- (iii) Due to a potential separation of around 300 mV between the two pairs of symmetric peaks, the specific energy gain delivered at the discharge at 1 A g^{-1} almost tripled by using triisopropylsilyl protecting groups, compared to the methyl groups.
- (iv) The different locations in potential of the reversible electrochemical systems obtained in cyclic voltammetry seem mainly due to a textural effect. A tenable explanation is that the protection of catechol with bulky silyl groups does not allow the diffusion of the diazonium salt in the microporosity, while the 3,4-dimethoxybenzenediazonium salt can

have access to a part of the micropores and can possibly reduce their volume by a progressive coverage of their inner surface.

The protection/deprotection strategy reported here could offer the possibility of matching a more important energy to the faradaic contribution of the electric charge storage in pseudo-supercapacitors just by adapting the textural properties of the activated carbon to the molecular size, without multi-step synthesis to prepare selected molecules.

Acknowledgment

This work was supported by the Centre National de la Recherche Scientifique (CNRS-France) through the framework of the ICROSS project (ANR-13-PRGE-0011-02). We also thanks the French Ministry for the PhD grant of E. Touzé.

Appendix A. Supplementary data

Supplementary data related to this article can be found at <https://doi.org/10.1016/j.electacta.2018.01.115>.

References

- [1] K.W. Leitner, B. Gollas, M. Winter, J.O. Besenhard, Combination of redox capacity and double layer capacitance in composite electrodes through immobilization of an organic redox couple on carbon black, *Electrochim. Acta* 50 (2004) 199–204.
- [2] S. Isikli, R. Diaz, Substrate-dependent performance of supercapacitors based on an organic redox couple impregnated on carbon, *J. Power Sources* 206 (2012) 53–58.
- [3] R.D.L. Smith, P.G. Pickup, Novel electroactive surface functionality from the coupling of an aryl diamine to carbon black, *Electrochem. Commun.* 11 (2009) 10–13.
- [4] Z. Algharaibeh, X. Liu, P.G. Pickup, An asymmetric anthraquinone-modified carbon/ruthenium oxide supercapacitor, *J. Power Sources* 187 (2009) 640–643.
- [5] K. Kalinathan, D.P. DesRoches, X. Liu, P.G. Pickup, Anthraquinone modified carbon fabric supercapacitors with improved energy and power densities, *J. Power Sources* 181 (2008) 182–185.
- [6] M. Weissmann, O. Crosnier, T. Brousse, D. Bélanger, Electrochemical study of anthraquinone groups, grafted by the diazonium chemistry, in different aqueous media-relevance for the development of aqueous hybrid electrochemical capacitor, *Electrochim. Acta* 82 (2012) 250–256.
- [7] L. Madec, A. Bouvrée, P. Blanchard, C. Cougnon, T. Brousse, B. Lestriez, D. Guyomard, J. Gaubicher, In situ redox functionalization of composite electrodes for high power–high energy electrochemical storage systems via a non-covalent approach, *Energy Environ. Sci.* 5 (2012) 5379–5386.
- [8] E. Lebègue, T. Brousse, O. Crosnier, J. Gaubicher, C. Cougnon, Direct introduction of redox centers at activated carbon substrate based on acid-substituent-assisted diazotization, *Electrochem. Commun.* 25 (2012) 124–127.
- [9] E. Lebègue, T. Brousse, J. Gaubicher, C. Cougnon, Chemical functionalization of activated carbon through radical and diradical intermediates, *Electrochem. Commun.* 34 (2013) 14–17.
- [10] S. Isikli, M. Lecea, M. Ribagorda, M.C. Carreno, R. Diaz, Influence of quinone grafting via Friedel–Crafts reaction on carbon porous structure and supercapacitor performance, *Carbon* 66 (2014) 654–661.
- [11] G. Pognon, T. Brousse, L. Demarconnay, D. Bélanger, Performance and stability of electrochemical capacitor based on anthraquinone modified activated carbon, *J. Power Sources* 196 (2011) 4117–4122.
- [12] A. Le Comte, G. Pognon, T. Brousse, D. Bélanger, Determination of the quinone-loading of a modified carbon powder-based electrode for electrochemical capacitor, *Electrochemistry* 81 (2013) 863–866.
- [13] Q. Abbas, P. Ratajczak, P. Babuchowska, A. Le Comte, D. Bélanger, T. Brousse, F. Béguin, Strategies to improve the performance of carbon/carbon capacitors in salt aqueous electrolytes, *J. Electrochem. Soc.* 162 (2015) A5148–A5157.
- [14] X. Chen, H. Wang, H. Yi, X. Wang, X. Yan, Z. Guo, Anthraquinone on porous carbon nanotubes with improved supercapacitor performance, *J. Phys. Chem. C* 118 (2014) 8262–8270.
- [15] A. Le Comte, T. Brousse, D. Bélanger, Simpler and greener grafting method for improving the stability of anthraquinone-modified carbon electrode in alkaline media, *Electrochim. Acta* 137 (2014) 447–453.
- [16] C. Cougnon, E. Lebègue, G. Pognon, Impedance spectroscopy study of a catechol-modified activated carbon electrode as active material in electrochemical capacitor, *J. Power Sources* 274 (2015) 551–559.
- [17] Z. Algharaibeh, P.G. Pickup, An asymmetric supercapacitor with anthraquinone and dihydroxybenzene modified carbon fabric electrodes, *Electrochem. Commun.* 13 (2011) 147–149.
- [18] E. Lebègue, T. Brousse, J. Gaubicher, R. Retoux, C. Cougnon, Toward fully organic rechargeable charge storage devices based on carbon electrodes grafted with redox molecules, *J. Mater. Chem.* 2 (2014) 8599–8602.
- [19] N. An, Y. An, Z. Hu, B. Guo, Y. Yang, Z. Lei, Graphene hydrogels non-covalently functionalized with alizarin: an ideal electrode material for symmetric supercapacitors, *J. Mater. Chem.* 3 (2015) 22239–22246.
- [20] X. Su, K.-J. Tan, J. Elbert, C. Rüttiger, M. Gallei, T.F. Jamison, T.A. Hatton, Asymmetric Faradaic systems for selective electrochemical separations, *Energy Environ. Sci.* 10 (2017) 1272–1283.
- [21] C. Karlsson, E. Jämstorp, M. Strømme, M. Sjödin, Computational electrochemistry study of 16 isoindole-4,7-diones as candidates for organic cathode materials, *J. Phys. Chem. C* 116 (2012) 3793–3801.
- [22] K. Hernandez-Burgos, S.E. Burkhardt, G.G. Rodríguez-Calero, R.G. Hennig, H.D. Abruña, Theoretical studies of carbonyl-based organic molecules for energy storage applications: the heteroatom and substituent effect, *J. Phys. Chem. C* 118 (2014) 6046–6051.
- [23] R.B. Araujo, A. Banerjee, P. Panigrahi, L. Yang, M. Strømme, M. Sjödin, C.M. Araujo, R. Ahuja, Designing strategies to tune reduction potential of organic molecules for sustainable high capacity battery application, *J. Mater. Chem.* 5 (2017) 4430–4454.
- [24] S.E. Burkhardt, M.A. Lowe, S. Conte, W. Zhou, H. Qian, G.G. Rodríguez-Calero, J. Gao, R.G. Hennig, H.D. Abruña, Tailored redox functionality of small organics for pseudocapacitive electrodes, *Energy Environ. Sci.* 5 (2012) 7176–7187.
- [25] G. Pognon, C. Cougnon, D. Mayilukila, D. Bélanger, Catechol-modified activated carbon prepared by the diazonium chemistry for application as active electrode material in electrochemical capacitor, *ACS Appl. Mater. Interfaces* 4 (2012) 3788–3796.
- [26] S. Uchiyama, H. Watanabe, H. Yamazaki, A. Kanazawa, H. Hamana, Y. Okabe, Electrochemical introduction of amino group to a glassy carbon surface by the electrolysis of carbamic acid, *J. Electrochem. Soc.* 154 (2007) F31–F35.
- [27] G.G. Wildgoose, A.T. Masheter, A. Crossley, J.H. Jones, R.G. Compton, Electrolysis of ammonium carbamate: a voltammetric and X-ray photoelectron spectroscopic investigation into the modification of carbon electrodes, *Int. J. Electrochem. Sci.* 2 (2007) 809–819.
- [28] T. Nagaoka, T. Yoshino, Surface properties of electrochemically pretreated glassy carbon, *Anal. Chem.* 58 (1986) 1037–1042.
- [29] A.S. Kumar, S. Sornambikai, P. Gayathri, J.-M. Zen, Selective covalent immobilization of catechol on activated carbon electrodes, *J. Electroanal. Chem.* 641 (2010) 131–135.
- [30] A.S. Kumar, P. Swetha, Electrochemical-assisted encapsulation of catechol on a multiwalled carbon nanotube modified electrode, *Langmuir* 26 (2010) 6874–6877.
- [31] S.A. Trammell, M. Moore, T.L. Schull, N. Lebedev, Synthesis and electrochemistry of self-assembled monolayers containing quinone derivatives with varying electronic conjugation, *J. Electroanal. Chem.* 628 (2009) 125–133.
- [32] N.H. Nguyen, C. Cougnon, F. Gohier, Deprotection of arenediazonium tetrafluoroborate ethers with BBr₃, *J. Org. Chem.* 74 (2009) 3955–3957.
- [33] M. Li, S.M.D. Shandilya, M.A. Carpenter, A. Rathore, W.L. Brown, A.L. Perkins, D.A. Harki, J. Solberg, D.J. Hook, K.K. Pandey, M.A. Parniak, J.R. Johnson, N.J. Krogan, M. Somasundaran, A. Ali, C.A. Schiffer, R.S. Harris, First-in-class small molecule inhibitors of the single-strand DNA cytosine deaminase APOBEC3G, *ACS Chem. Biol.* 7 (2012) 506–517.
- [34] W.G. Hong, B.H. Kim, S.M. Lee, H.Y. Yu, Y.J. Yun, Y. Jun, J.B. Lee, H.J. Kim, Agent-free synthesis of graphene oxide/transition metal oxide composites and its application for hydrogen storage, *Int. J. Hydrogen Energy* 37 (2012) 7594–7599.
- [35] A. Pendashteh, M.F. Mousavi, M.S. Rahmanifar, Fabrication of anchored copper oxide nanoparticles on graphene oxide nanosheets via an electrostatic coprecipitation and its application as supercapacitor, *Electrochim. Acta* 88 (2013) 347–357.
- [36] M. Andresen, L.-S. Johansson, B.S. Tanem, P. Stenius, Properties and characterization of hydrophobized microfibrillated cellulose, *Cellulose* 13 (2006) 665–677.
- [37] Y.R. Leroux, H. Fei, J.-M. Noël, C. Roux, P. Hapiot, Efficient covalent modification of a carbon surface: use of a silyl protecting group to form an active monolayer, *J. Am. Chem. Soc.* 132 (2010) 14039–14041.
- [38] M. Toupin, D. Bélanger, Thermal stability study of aryl modified carbon black by in situ generated diazonium salt, *J. Phys. Chem. C* 111 (2007) 5394–5401.
- [39] P. Doppelt, G. Hallais, J. Pinson, F. Podvorica, S. Verneyre, Surface modification of conducting substrates. Existence of azo bonds in the structure of organic layers obtained from diazonium salts, *Chem. Mater.* 19 (2007) 4570–4575.
- [40] B.L. Hurlley, R.L. McCreery, Covalent bonding of organic molecules to Cu and Al alloy 2024 T3 surfaces via diazonium ion reduction, *J. Electrochem. Soc.* 151 (2004) B252–B259.
- [41] L. Madec, K.A. Seid, J.-C. Badot, B. Humbert, P. Moreau, O. Dubrunfaut, B. Lestriez, D. Guyomard, J. Gaubicher, Redirected charge transport arising from diazonium grafting of carbon coated LiFePO₄, *Phys. Chem. Chem. Phys.* 16 (2014) 22745–22753.
- [42] G. Liu, E. Luais, J.J. Gooding, The fabrication of stable gold nanoparticle-modified interfaces for electrochemistry, *Langmuir* 27 (2011) 4176–4183.
- [43] P. Brant, R.D. Feltham, X-ray photoelectron spectra of aryl diazo derivatives of transition metals, *J. Organomet. Chem.* 120 (1976) C53–C57.

- [44] P. Finn, W.-L. Jolly, Nitrogen 1s binding energies of some azide, dinitrogen, and nitride complexes of transition metals, *Inorg. Chem.* 11 (1972) 1434–1435.
- [45] T.M. Bockman, D. Kosynkin, J.K. Kochi, Isolation and structure elucidation of transient (colored) complexes of arenediazonium with aromatic hydrocarbons as intermediates in arylations and azo couplings, *J. Org. Chem.* 62 (1997) 5811–5820.
- [46] T. Menanteau, M. Dias, E. Levillain, A.J. Downard, T. Breton, Electrografting via diazonium chemistry: the key role of the aryl substituent in the layer growth mechanism, *J. Phys. Chem. C* 120 (2016) 4423–4429.
- [47] Y. Xie, P.M.A. Sherwood, X-ray photoelectron spectroscopic studies of carbon fiber surfaces. Differences in the surface chemistry and bulk structure of different carbon fibers based on poly(acrylonitrile) and pitch and comparison with various graphite samples, *Chem. Mater.* 2 (1990) 293–299.
- [48] Y.R. Leroux, P. Hapiot, Nanostructured monolayers on carbon substrates prepared by electrografting of protected aryldiazonium salts, *Chem. Mater.* 25 (2013) 489–495.
- [49] J. Lehr, B.E. Williamson, A.J. Downard, Spontaneous grafting of nitrophenyl groups to planar glassy carbon substrates: evidence for two mechanisms, *J. Phys. Chem. C* 115 (2011) 6629–6634.
- [50] K.S.W. Sing, D.H. Everett, R.A.W. Haul, L. Moscou, R.A. Pierotti, J. Rouquerol, T. Siemieniewska, *Pure Appl. Chem.* 57 (1985) 603–619.
- [51] G. Pognon, T. Brousse, D. Belanger, Effect of molecular grafting on the pore size distribution and the double layer capacitance of activated carbon for electrochemical double layer capacitors, *Carbon* 49 (2011) 1340–1348.